ACS Catalysis

pubs.acs.org/acscatalysis

Research Article

Electronic Interactions between Anchored Molecular Catalyst and Support

Stephanie A. Johnson,[†] James R. Wilkes,[†] Dunwei Wang,* and Jeffery A. Byers*

Cite This: *ACS Catal.* 2024, 14, 18535−18541

Read Online

ACCESS | Metrics & More | Article Recommendations | Supporting Information

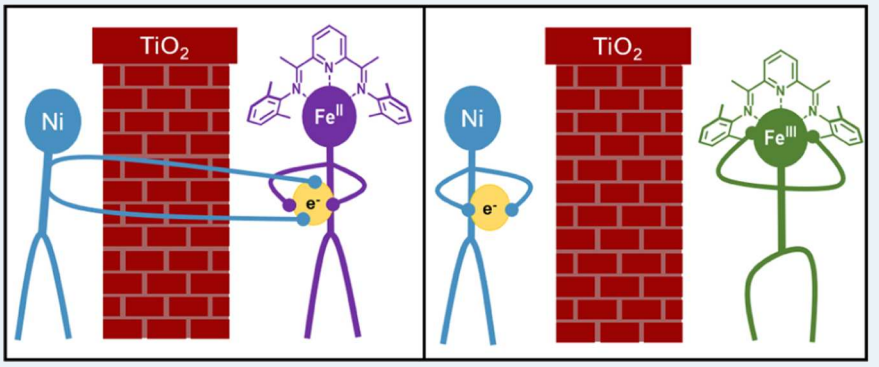

ABSTRACT: Immobilizing molecular catalysts on surfaces introduces spatial control of catalysis and promises improved stability and recyclability of the catalyst. The interplays between the support and the immobilized molecular species, however, remain underexplored. Using Ni as a prototypical support, here we report a study on how the electronic interactions between the support and the molecular catalyst impacts the reactivity. This work was built upon our previous successes in switching the reactivity of iron bis(iminopyridine) alkoxide complexes through redox toggling, where the anchored iron(II) complex polymerizes lactide, and its cationic iron(III) counterpart polymerizes epoxides. It was found that Ni as a metal support could readily oxidize the complex to exhibit catalytic activity toward epoxide polymerization. The charge transfer between Ni and the Fe complex could be modulated by either electrochemical reduction or adding a layer of TiO_2. The results are expected to have major implications for research efforts aimed at converging homogeneous and heterogeneous catalysis.

KEYWORDS: *catalysis, polymerization, semiconductors, surface science, oxidation state*

INTRODUCTION

Growing research attention has recently been attracted to catalysis using immobilized molecular catalysts on solid-state supports.[1−3] The main purported benefit of such an approach is to capitalize on the advantages of both homogeneous and heterogeneous catalysts. For the former, superior performance in terms of chemo-, regio-, and stereoselectivity is expected thanks to the advancement of molecular science; for the latter, improved recyclability and durability are key advantages to be expected. Indeed, exciting progress has already been made in the fields of dye-sensitized solar cells,[4] solar fuel synthesis,[5] and electrocatalysis,[6] among others. While early research has mostly treated the support as chemically inert, a growing body of work has pointed to the fact that the interactions between the catalytic moiety and the support may exert a profound influence on the overall reactivity.[7,8] Consider recent work by Surendranath et al. as an example. It was demonstrated that proton-coupled electron transfer could be promoted by rhenium catalysts conjugated to graphite electrodes under electrocatalytic conditions.[9,10] Similarly, Baik et al. have reported that the electron donating and withdrawing properties of the support may be tuned by varying the applied potentials, thereby controlling the reactivity of an anchored substrate for Suzuki-Miyaura cross-coupling.[11] It has become clear that the supporting substrate could be treated as a ligand, which, through the application of external potentials, impacts the reactivity of the active site through electronic and steric effects. How the catalytic activity of an immobilized molecular catalyst is altered by the inherent electronic properties of the supporting substrate remains underexplored.[12] This is in stark contrast to the large body of literature on similar studies concerning the so-called metal−support interactions (MSI) that play important roles in metal-cluster-based heterogeneous catalysts.[13−16] The work reported

Received: September 27, 2024
Revised: November 24, 2024
Accepted: November 26, 2024
Published: December 5, 2024

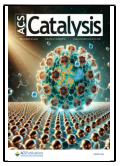

https://doi.org/10.1021/acscatal.4c05947
ACS Catal. 2024, 14, 18535−18541

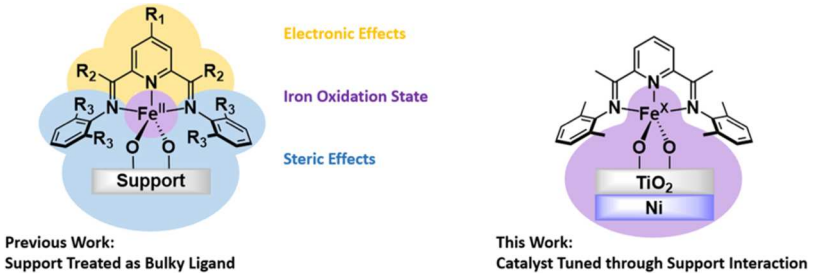

Figure 1. (Left): Previous work wherein the electronic effect of the support was underexplored. (Right): This work wherein support electronic effects are examined.

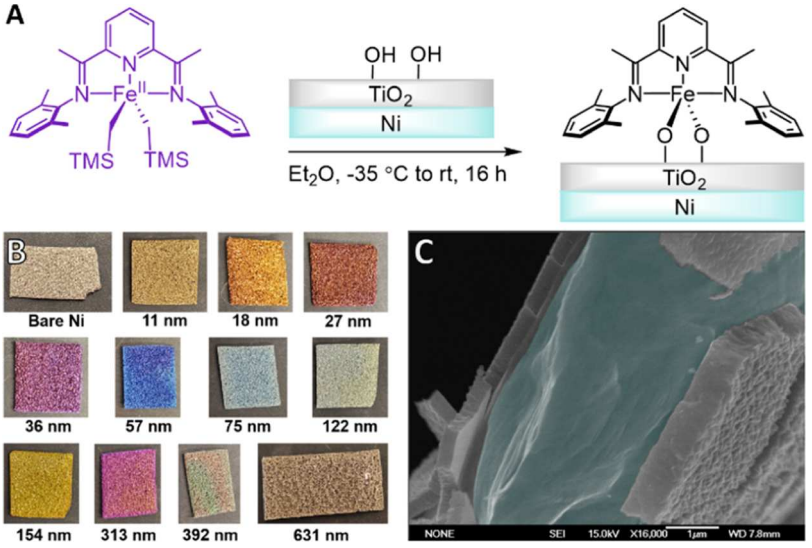

Figure 2. (A) Scheme of the Fe Anchoring Strategy. (B) Photo of TiO_2/Ni, showcasing the photonic effect due to the varying TiO_2 thicknesses. (C) SEM Image of Fe@TiO_2/Ni-631. The image was false colored to highlight the Ni (green blue) and the TiO_2 shell (gray). Image taken at a cracking point due cutting the sample during preparation, where the Ni was exposed for viewing convenience.

here is conceived to fill this knowledge gap. It was discovered that there is a strong electronic interaction between the supporting substrate and a prototypical Fe-based molecular catalyst. The effect only became obvious when Ni was used as a support, and it can be readily tuned by separating the molecular moiety from the Ni support through changing the thickness of an oxide interlayer.

Here we chose iron bis(iminopyridine) complexes as a prototypical molecular catalyst for the present study. Our previous research has revealed that the catalyst exhibits switchability toward the polymerization of lactide or epoxide: in its reduced form, the catalyst is active for lactide polymerization but inactive for epoxide polymerization; in its oxidized form, an opposite reactivity is observed.[17,18] The orthogonal reactivity and the ability to readily switch between the two states make this catalyst an excellent candidate for reactions such as the synthesis of sequence-controlled polymers from mixed monomers. Importantly, it has been shown by our previous work that the switch of the reactivity may be achieved with chemical reductants/oxidants[18] or through electrochemistry,[19] in homogeneous forms or as immobilized catalysts,[20] highlighting the versatility and reliability of this system. Nevertheless, for immobilization our previous work has only used oxides (TiO_2) as a support. As a semiconductor, TiO_2 features a gap in its energy states, within which the redox potential of the Fe complex resides. As such, minimum charge transfer is expected between the support and the catalytic moiety in the absence of externally applied potentials (or light). While such a property is desired from a stability perspective, it would be interesting to ask what happens if a different support were employed, such as one featuring continuous density of states like a metal. It is within this context that we carried out the current study. Our primary goal was to investigate the electronic interactions between the supporting substrate and the catalytic moiety. For this purpose, we employed Ni foam as a support to take advantage of its good conductivity, high surface area, and the fact that it features a continuous density of states with a workfunction more positive than the redox potential of the Fe complex. It was observed that electron transfer readily took place from the Fe complex to the Ni support, resulting in oxidation of the complex as evidenced by its exclusive reactivity toward epoxide polymerization. When separated from the support by a TiO_2 layer, the oxidation of the Fe complex was less pronounced, and the resulting immobilized catalysts showed decreasing reactivity toward epoxide polymerization with increasing TiO_2 thickness, which is accompanied by an increasing degree of reactivity toward lactide polymerization depending on the thickness of TiO_2.

RESULTS AND DISCUSSION

To study the effect of the support on anchored redox-active catalysts, iron bis(iminopyridine) complexes were tethered to Ni foams with TiO_2 coating (TiO_2/Ni, Figure 1). TiO_2/Ni

https://doi.org/10.1021/acscatal.4c05947
ACS Catal. 2024, 14, 18535−18541

foams of varying TiO_2 thickness (0−631 nm) were prepared using atomic layer deposition (ALD) and treated with ozone under ultraviolet (UV) light to increase the surface hydroxyl content, which was found to facilitate the immobilization of the Fe complexes. Uniform deposition of TiO_2 onto porous substrates using ALD has previously been demonstrated.[21] The TiO_2 thickness was measured by ellipsometry on a control substrate that was made of planar Si and was placed side-by-side with the Ni foam during the ALD process. For TiO_2 coatings >500 nm, the thickness was measured using scanning electron microscopy (SEM). Our initial studies focused on iron(II) bis(iminopyridine) complexes, which were anchored through a protonolysis reaction to produce Fe@TiO_2/Ni-*X*, where *X* denotes the thickness of the TiO_2 coating (Figure 2). The photonic effects of the varying TiO_2 thickness were apparent from the vibrant colors of the substrate, as shown in Figure 2B, further supporting the successes in preparing substrates with uniform TiO_2 coatings of varying thicknesses. No decomposition of the Fe complex was detected after anchoring, as determined by the absence of ligand in the supernatant after washing. When anchored on nanoparticulate TiO_2 that is white in color, the reduced form of the complex appears purple, and the oxidized form would be green. Due to the vibrant colors of the TiO_2/Ni supports, however, it was difficult to directly observe and compare the color changes expected from the presence of the Fe complex. The Fe loading was determined by inductively coupled plasma optical emission spectroscopy (ICP-OES) to be 0.0034 ± 0.0018 wt % Fe.

Our previous work has confirmed using Mössbauer spectroscopy that Fe primarily exhibits a 2^+ formal charge in the reduced form, whereas its oxidation state is formally 3^+ in the oxidized form. In this work, we employed X-ray photoelectron spectroscopy (XPS) to probe the oxidation state of Fe on TiO_2/Ni foams with varying TiO_2 thicknesses. This characterization was enabled by a vacuum sample transfer module that prevented air exposure of the samples to be transferred. As such, the XPS spectra reports on the chemical states of Fe in its innate forms. The spectra between 50 and 60 eV were collected and analyzed which correspond to the binding energies of Fe 3p electrons.[22] To establish a baseline for this set of characterizations, we first examined the molecular iron bis(iminopyridine) alkoxide complexes in its dry form by XPS (Figure S11).

Peak deconvolution revealed that only Fe^{2+} species were present, consistent with our previous Mössbauer characterizations. By comparison, only Fe^{3+} species were detected when Fe complexes were anchored onto the NiO layer of uncoated Ni foam, as shown in Figure S1. The same was true for Ni supports with <100 nm TiO_2 coating (Figure 3). For samples with >100 nm TiO_2 coating, a mixture of Fe^{2+} and Fe^{3+} species was observed, as shown in several prototypical spectra in Figure 3. For ease of comparisons and to highlight the differences, selected spectra of Fe@TiO_2/Ni-36, Fe@TiO_2/Ni-217, Fe@TiO_2/Ni-392, and Fe@TiO_2/Ni-631 are plotted in Figure 3, and the peaks were deconvoluted into those of Fe^{2+} and Fe^{3+} as follows. The peak attributed to Fe^{3+} centers at ca. 55.1 eV, and that to Fe^{2+} centers at ca. 53.6 eV. In all cases where TiO_2 was grown by ALD, no Ni was detected by XPS, supporting successful and complete TiO_2 coverage. Once the thickness of the ALD TiO_2 coating reached 631 nm, the percentage of Fe^{2+} increased to 28%. Due to the nature of slow growth by ALD, we did not attempt to further increase TiO_2 thickness by ALD. Rather, a sol−gel method was employed to prepare thicker (5−7 μm) TiO_2 on Ni foam. This thick TiO_2 coating is expected to block any electronic effects by the Ni support on the Fe complexes. Indeed, the highest Fe^{2+} content (89%) was measured on this sample (Figure 4). For comparison purposes, a similar Fe^{2+} content (82%) was measured on Fe@TiO_2−NPs. This value is in good agreement with our previously reported Mössbauer data.[20] We hypothesize that the presence of a small but persistent portion of Fe^{2+} (up to 20%) in the iron bis(iminopyridine) complexes in its

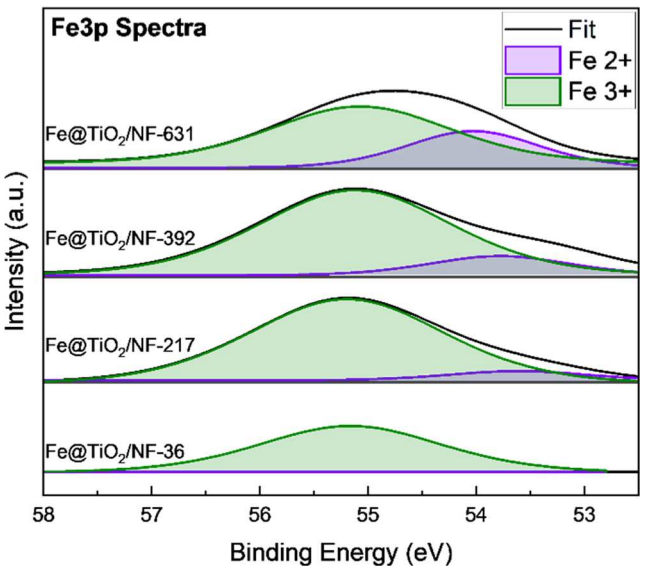

Figure 3. XPS spectra reporting the binding energies of Fe 3p electrons. From bottom to top: Fe@TiO_2/Ni-36, Fe@TiO_2/Ni-217, Fe@TiO_2/Ni-392, and Fe@TiO_2/Ni-631. Peak deconvolution was carried out to highlight contributions by two key species, Fe^{2+} (light purple) and Fe^{3+} (light green). The peak corresponding to the Fe^{2+} state of the catalyst increases as the thickness of ALD grown TiO_2.

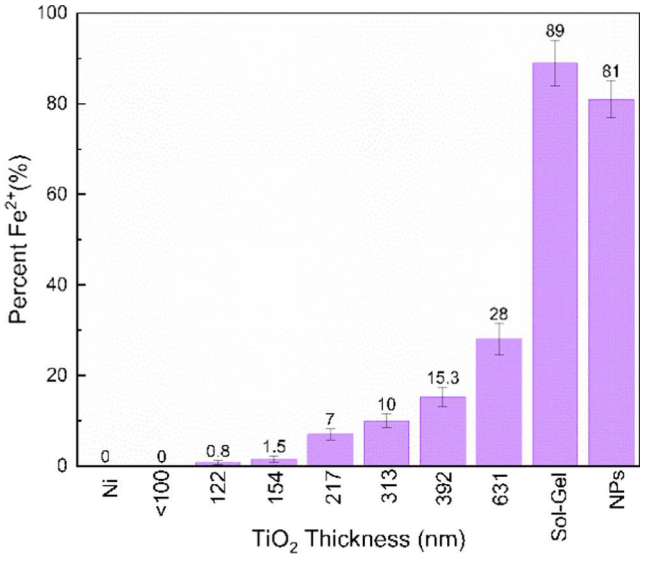

Figure 4. Fe^{2+} content measured on Ni foam with varying TiO_2 thicknesses, including no TiO_2, ALD grown (label on *x*-axis denotes thickness in nm), Sol−Gel prepared and TiO_2 NP. Error bars were calculated by calculating the standard deviation of all the samples with that thickness (3 measurements per sample).

https://doi.org/10.1021/acscatal.4c05947
ACS Catal. 2024, 14, 18535−18541

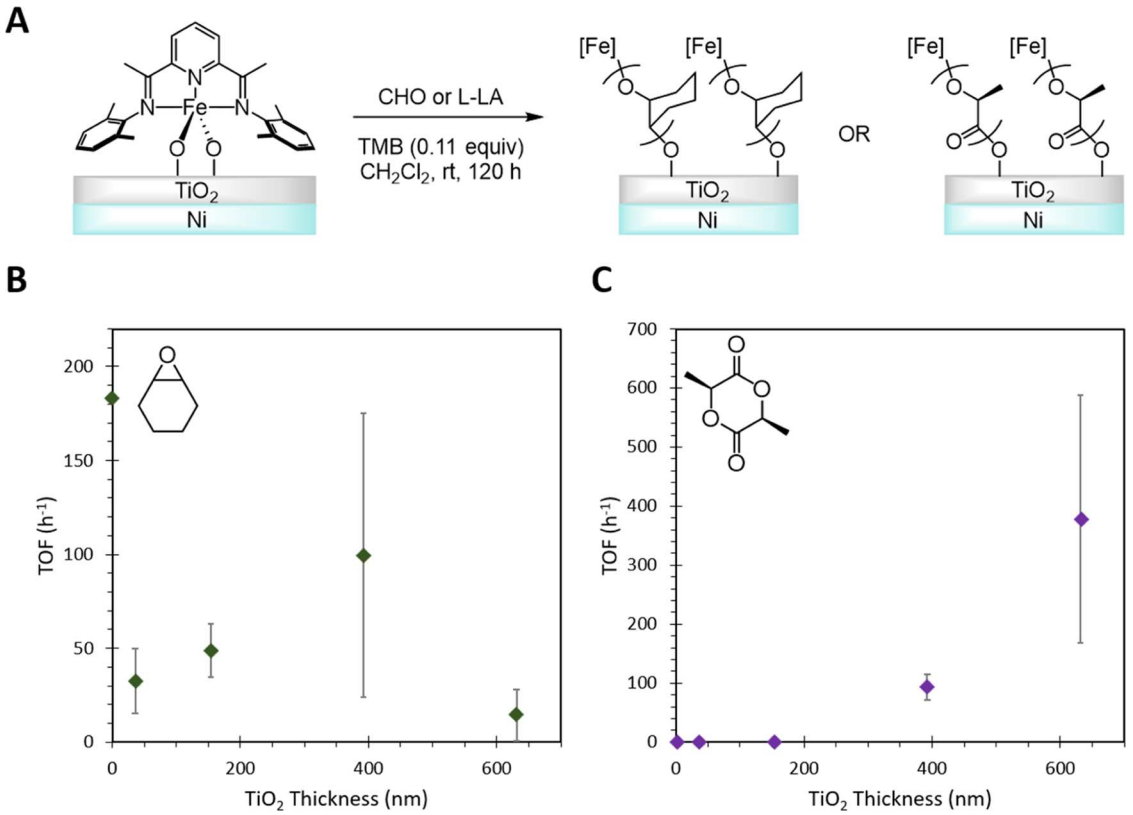

Figure 5. Effect of TiO_2 thickness on TOF for CHO and L-LA polymerizations on Fe@TiO_2/Ni foams prepared via ALD. (A) Scheme of polymerization reactions using CHO or L-LA monomers. (B) Comparison of Fe reactivity for CHO polymerizations at different TiO_2 thicknesses (C) Comparison of Fe reactivity for L-LA polymerizations at different TiO_2 thicknesses.

anchored forms on TiO_2 is a result of direct electron transfer from the complex to the valence band of TiO_2. Such a transfer may be regarded as recombination between electrons from the Fe complex and holes in TiO_2. Because holes in TiO_2 are a minority carrier, their concentrations are low in the dark. As such, oxidation is limited. Supporting this hypothesis was the observation that exposure to light led to a greater degree of oxidation of the complexes, which accelerated its degradation. To fully resolve the reasons behind this effect, namely a persistent presence of a small portion of oxidized complexes, would likely require additional research that is beyond the scope of the current work.

With the complexes successfully anchored and characterized, our next task was to determine whether the support effects altered the reactivity of the anchored iron catalysts. For this task, the Fe@TiO_2/Ni foams were employed as polymerization catalysts, with the reactions monitored by consumption of the monomer compared to an internal standard (1,3,5-trimethoxybenzene, TMB) using proton nuclear magnetic resonance (^{1}H NMR) (Table S1 and Figure 5). Turnover frequency (TOF) was calculated using the amount of active Fe catalyst as determined from ICP-OES and XPS. We first ensured that the Ni supports themselves were not active for polymerization; we observed no conversion of monomer for either cyclohexene oxide (CHO) or L-lactide (L-LA) when no Fe was present.

We expected that foams with thinner TiO_2 coatings would be capable of epoxide polymerization due to the greater proportion of Fe^{3+} present. When Fe@TiO_2/Ni-36 was exposed to a solution containing CHO, polymerization proceeded, although slowly compared to Fe^{3+}@TiO_2 nanoparticles presumably due to the lower Fe loading of the former. When Fe@TiO_2/Ni-631 was used as the catalyst, epoxide polymerization was still observed at comparable rates, which was consistent with our XPS results that Fe^{3+} still accounted for 72% of all Fe content on this support. Epoxide polymerization is not turned off until high concentration of Fe^{2+} is achieved, as observed on the Ni foam with sol−gel TiO_2 coating (89% Fe^{2+}) and Fe^{2+}@TiO_2 nanoparticle (81% Fe^{2+}) supports.

In contrast, when L-LA polymerization was attempted using Fe@TiO_2/Ni-36, no polymerization occurred. This result was expected, as XPS characterizations showed no Fe^{2+} on the support. The highest conversion of L-LA on ALD-coated Ni foams was achieved with Fe@TiO_2/Ni-631 (Figure 5; see Supporting Information for tabulated data). These results were in line with the expectations based on XPS results. Foams with less than 15% Fe^{2+} content were unable to catalyze L-LA polymerization. When Fe^{2+} constituted a significant, albeit still minor, proportion of the Fe present, L-LA polymerization was switched on. We anticipate that this trend would hold for even thicker TiO_2 layers; nevertheless, thicker TiO_2 coatings were not synthesized systematically by ALD beyond 631 nm due to the inefficiencies of synthesis by ALD for thick films. Additionally, attempts to isolate the polymer from the surface were unsuccessful due to the small amount of polymer formed.

Next, we turned our attention to studying the reduction of the Fe^{3+} catalyst to verify its switchability. Chemical reduction through the addition of cobaltocene was explored on Fe@TiO_2/Ni-36. The reactions were setup similarly to those discussed previously, except with a large excess of cobaltocene (5 μmol) present. L-LA conversion reached 23%, demonstrating that when the Fe complex was reduced, its reactivity

https://doi.org/10.1021/acscatal.4c05947
ACS Catal. 2024, 14, 18535−18541

toward PLA polymerization was preserved. The result strongly supports that the molecular identity of the catalyst was preserved; furthermore, the catalyst exhibited switchability. We note that the reaction rate is too slow for practical polymerization application, and there should be significant room for further improvement in terms of conversions and the reaction rates. For instance, the loading of catalyst could be further increased to accelerate the reactions. Nevertheless, the results served as encouraging proof of concept, and they support the switchability of the Fe complex was intact in the anchored form. Most importantly, the results highlight the oxidation of the Fe complex by the Ni support, which could be reversed by the application of a reductant.

CONCLUSIONS

In summary, we explored the support effects of heterogeneous molecular catalysis and demonstrated that strong electronic interactions between the support and the molecular moiety could have a profound impact on the reactivity of the catalytic center. That Ni as a metal support readily oxidized the Fe complex was a surprise with no similar reports in the literature, to the best of our knowledge. It was shown that this electronic interaction could be tuned by controlling the thickness of an insulating layer, the TiO_2 coating. It was further found that the thinner the TiO_2 layer on the nickel foams, the more oxidation the iron bis(iminopyridine) complex underwent. As the TiO_2 layers on the foams increased, less oxidation occurred, and more Fe^{2+} was present. Encouragingly, the chemical nature of the catalyst appeared unchanged, so was its ability to switch reactivity in response to the changes in oxidation states. The electronic communication between the molecular catalyst and its support highlights the importance of matching the inherent electronic properties of the support when used as a ligand for an anchored molecular catalyst. The ability to tune the reactivity of the catalytic center through controlling the electronic properties of the support, either through electrochemical, chemical, photo, or even magnetic means open new doors to control catalysis.

METHODS

Preparation of TiO_2-Coated Ni Foams Using ALD. Nickel foam was cut into 1 × 3 cm^2 rectangles and cleaned by sequential sonication in water, acetone, and isopropyl alcohol, then dried with compressed air. The foams were then coated by ALD (Cambridge NanoTech Savannah 100) through iterative exposure of titanium(IV) isopropoxide and water. ALD was cycled between 500 and 20,000 cycles to achieve various thicknesses. The deposition temperature for ALD was 275 °C and pulsed consisted of 0.01s pulse of H_2O, 10s purge, 0.1s pulse titanium(IV) isopropoxide, 7s purge, and repeated for *X* number of cycles. After ALD, a 30 min UV ozone treatment of the foams was used to increase surface hydroxyl content. Ellipsometry (Woolam WVASE) was performed on a silica wafer included in each batch of foams to determine the approximate thickness of the TiO_2 layer on the Ni. SEM images further corroborated the presence and thickness of the TiO_2 layer (Figure S17)

Preparation of Titania-Coated Nickel Foams through Sol−Gel Method. Nickel foam was cut into 1 × 3 cm^2 rectangles, cleaned by sequential sonication in water, acetone, and isopropyl alcohol, then dried with compressed air. In a 20 mL vial, titanium(IV) isopropoxide (1 mL) and ethanol (4 mL) were mixed. The Ni foams were then submerged in the solution for 2 h. After 2 h, the resultant TiO_2/Ni foams were dried in vacuo overnight, then rinsed with ethanol. A 30 min ultraviolet (UV) ozone treatment was performed on the TiO_2/Ni foams upon drying.

Anchoring of Iron Complexes onto Titania-Coated Nickel Foams. TiO_2/Ni foams were dried under reduced pressure at 100 °C, then brought into an N_2-filled glovebox. The TiO_2/Ni foams were soaked in a solution of bis(imino)-pyridine iron bisalkyl complex (150 mg, 0.24 mmol) in diethyl ether (12 mL) for 16 h. The foams were rinsed with diethyl ether (10 × 5 mL) until the resulting supernatant was colorless. Ligand was not observed in the supernatant after washing by ^{1}H NMR (ligand presence would indicate catalyst decomposition). Upon digestion in 1% nitric acid, ICP-OES (Agilent 5100) showed the iron concentration on the foams was 0.0034 ± 0.0018 wt % Fe.

Analysis of Samples with X-ray Photoelectron Spectroscopy. A vacuum-transfer module was used to transfer Fe@TiO_2/Ni foams from the glovebox to the vacuum of the XPS working chamber without exposure to noninert atmosphere. XPS was performed on a Thermofisher K Alpha XPS instrument (Al kα X-ray radiation). Data treatment for the XPS spectra was performed in Avantage software and multiple regions of binding energies were collected. For all spectra, a smart baseline was fit (a common baseline used for data analysis in Avantage). The primary analysis was between 50 and 60 eV, a region corresponding to Fe 3p electrons. A typical Fe 3p spectrum was fit with a Lorentzian (40%)−Gaussian (60%) function and a full width at half-maximum (fwhm) of 2.2 eV for Fe^{3+} and 1.6 eV for Fe^{2+}. The peak attributed to Fe^{3+} centers at 55.1 ± 0.1 eV while the peak attributed to Fe^{2+} centers at 53.6 ± 0.15 eV. Due to the complex satellite features in Fe 2p spectra, that region (710−740 eV) was collected, but not analyzed. The region corresponding to Ni 2p (850−890 eV) was also collected for each sample as a control, as for complete TiO_2 covered samples, Ni was not present at the surface, indicating complete coverage of the TiO_2 surface. Before the peak positions were compared, a charge correction to 284.8 eV for the peak corresponding to advantageous carbon in the C 1s spectra.

Polymerization of Cyclohexene Oxide on Fe@TiO_2/Ni Foams. In a 20 mL vial, cyclohexene oxide (125 mg, 1.3 mmol, 200 mM) and 1,3,5-trimethoxybenzene (23.7 mg, 0.14 mmol) were dissolved in dichloromethane (6.4 mL). The Fe@TiO_2/Ni foam and a stir bar were added to the vial. The reaction was allowed to stir vigorously at room temperature for up to 168 h. Aliquots were periodically removed from the monomer solution for ^{1}H NMR analysis (Varian 600 or 500 MHz Bruker Avance Neo spectrometer). Epoxide conversion was observed with ^{1}H NMR by comparing the relative integration of the methine peaks of the remaining cyclohexene oxide (*q*, 3.0 ppm) to the methyl peaks of the internal standard (*s*, 3.8 ppm). After the reaction, the Fe@TiO_2/Ni foam was washed with dichloromethane, then digested in 1% nitric acid for ICP-OES analysis. The TOF was calculated as follows: (moles of monomer converted)/(moles of Fe present × percent Fe^{3+} from XPS data)/reaction time = TOF

Polymerization of L-Lactide on Fe@TiO_2/Ni Foams. In a 20 mL vial, L-lactide (105 mg, 0.75 mmol, 100 mM) and 1,3,5-trimethoxybenzene (13.4 mg, 0.80 mmol) were dissolved in dichloromethane (6.9 mL). The Fe@TiO_2/Ni foam and a stir bar were added to the vial. The reaction was allowed to stir

https://doi.org/10.1021/acscatal.4c05947
ACS Catal. 2024, 14, 18535−18541

vigorously at room temperature for up to 168 h. For reactions performed in the presence of a reductant, $CoCp_2$ (1 mg, 5 μmol) was added. Aliquots were periodically removed from the monomer solution for ^{1}H NMR analysis. L-lactide conversion was observed with ^{1}H NMR, by comparing the relative integration of the methine peaks of the remaining L-lactide (*q*, 5.0 ppm) to the methyl peaks of the internal standard (*s*, 3.8 ppm). After the reaction, the Fe@TiO_2/Ni foam was washed with dichloromethane, then digested in 1% nitric acid for ICP-OES analysis. The TOF was calculated as follows: (moles of monomer converted)/(moles of Fe present × percent Fe^{2+} from XPS data)/reaction time = TOF.

■ ASSOCIATED CONTENT

Supporting Information

The Supporting Information is available free of charge at https://pubs.acs.org/doi/10.1021/acscatal.4c05947.

Experimental procedures as well as X-ray photoelectron spectra and cyclic voltammograms (PDF)

■ AUTHOR INFORMATION

Corresponding Authors

Dunwei Wang − *Department of Chemistry, Boston College, Chestnut Hill, Massachusetts 02467, United States;* orcid.org/0000-0001-5581-8799; Email: dunwei.wang@bc.edu

‡**Jeffery A. Byers** − *Department of Chemistry, Boston College, Chestnut Hill, Massachusetts 02467, United States;* orcid.org/0000-0002-8109-674X; Email: jeffery.byers@bc.edu

Authors

Stephanie A. Johnson − *Department of Chemistry, Boston College, Chestnut Hill, Massachusetts 02467, United States;* orcid.org/0009-0009-2673-5543

James R. Wilkes − *Department of Chemistry, Boston College, Chestnut Hill, Massachusetts 02467, United States;* orcid.org/0000-0002-7429-9362

Complete contact information is available at: https://pubs.acs.org/10.1021/acscatal.4c05947

Author Contributions

†S.A.J. and J.R.W. contributed equally to this work.

Notes

The authors declare no competing financial interest.

‡Professor J.A.B. died on August 18, 2023.

■ ACKNOWLEDGMENTS

This work was made possible by the Center of Integrated Catalysis, a program made possible by an NSF Center for Chemical Innovation Phase I grant (CHE-2023955). We thank the Boston College Electron Microscopy, Materials Characterization Core, Integrated Science Cleanroom, as well as Magnetic Resonance Center Facilities for assistance with the work presented in this paper. The authors would also like to thank Mr. Muchun Fei for his help in the SEM characterizations. NMR spectroscopy at BC was carried out in Merkert Chemistry Center NMR Core Laboratory and supported by the NSF MRI award CHE2117246 and the NIH HEI-S10 award 1S10OD026910-01A1.

■ REFERENCES

(1) Copéret, C.; Comas-Vives, A.; Conley, M. P.; Estes, D. P.; Fedorov, A.; Mougel, V.; Nagae, H.; Núñez-Zarur, F.; Zhizhko, P. A. Surface Organometallic and Coordination Chemistry toward Single-Site Heterogeneous Catalysts: Strategies, Methods, Structures, and Activities. *Chem. Rev.* **2016**, *116* (2), 323−421.

(2) Zaera, F. Designing Sites in Heterogeneous Catalysis: Are We Reaching Selectivities Competitive With Those of Homogeneous Catalysts? *Chem. Rev.* **2022**, *122* (9), 8594−8757.

(3) Samantaray, M. K.; Mishra, S. K.; Saidi, A.; Basset, J.-M. Surface Organometallic Chemistry: A Sustainable Approach in Modern Catalysis. *J. Organomet. Chem.* **2021**, *945*, No. 121864.

(4) Ayele, D. W.; Su, W.-N.; Rick, J.; Chen, H.-M.; Pan, C.-J.; Akalework, N. G.; Hwang, B.-J. Organometallic Compounds for Dye-Sensitized Solar Cells (DSSC). In *Advances in Organometallic Chemistry and Catalysis*; John Wiley & Sons, Ltd, 2013; pp 501−511.

(5) Whang, D. R. Immobilization of Molecular Catalysts for Artificial Photosynthesis. *Nano Convergence* **2020**, *7* (1), No. 37.

(6) Bullock, R. M.; Das, A. K.; Appel, A. M. Surface Immobilization of Molecular Electrocatalysts for Energy Conversion. *Chem. - Eur. J.* **2017**, *23* (32), 7626−7641.

(7) Witzke, R. J.; Chapovetsky, A.; Conley, M. P.; Kaphan, D. M.; Delferro, M. Nontraditional Catalyst Supports in Surface Organometallic Chemistry. *ACS Catal.* **2020**, *10* (20), 11822−11840.

(8) Copéret, C.; Fedorov, A.; Zhizhko, P. A. Surface Organometallic Chemistry: Paving the Way Beyond Well-Defined Supported Organometallics and Single-Site Catalysis. *Catal. Lett.* **2017**, *147* (9), 2247−2259.

(9) Oh, S.; Gallagher, J. R.; Miller, J. T.; Surendranath, Y. Graphite-Conjugated Rhenium Catalysts for Carbon Dioxide Reduction. *J. Am. Chem. Soc.* **2016**, *138* (6), 1820−1823.

(10) Jackson, M. N.; Surendranath, Y. Molecular Control of Heterogeneous Electrocatalysis through Graphite Conjugation. *Acc. Chem. Res.* **2019**, *52* (12), 3432−3441.

(11) Heo, J.; Ahn, H.; Won, J.; Son, J. G.; Shon, H. K.; Lee, T. G.; Han, S. W.; Baik, M.-H. Electro-Inductive Effect: Electrodes as Functional Groups with Tunable Electronic Properties. *Science* **2020**, *370* (6513), 214−219.

(12) Zhang, X.; Wolf, C.; Wang, Y.; Aubin, H.; Bilgeri, T.; Willke, P.; Heinrich, A. J.; Choi, T. Electron Spin Resonance of Single Iron Phthalocyanine Molecules and Role of Their Non-Localized Spins in Magnetic Interactions. *Nat. Chem.* **2022**, *14* (1), 59−65.

(13) Xu, M.; Peng, M.; Tang, H.; Zhou, W.; Qiao, B.; Ma, D. Renaissance of Strong Metal-Support Interactions. *J. Am. Chem. Soc.* **2024**, *146* (4), 2290−2307.

(14) Sang, K.; Zuo, J.; Zhang, X.; Wang, Q.; Chen, W.; Qian, G.; Duan, X. Towards a Molecular Understanding of the Electronic Metal-Support Interaction (EMSI) in Heterogeneous Catalysis. *Green Energy Environ.* **2023**, *8* (3), 619−625.

(15) Castro-Latorre, P.; Neyman, K. M.; Bruix, A. Systematic Characterization of Electronic Metal−Support Interactions in Ceria-Supported Pt Particles. *J. Phys. Chem. C* **2023**, *127* (36), 17700−17710.

(16) Shi, Y.; Ma, Z.-R.; Xiao, Y.-Y.; Yin, Y.-C.; Huang, W.-M.; Huang, Z.-C.; Zheng, Y.-Z.; Mu, F.-Y.; Huang, R.; Shi, G.-Y.; Sun, Y.-Y.; Xia, X.-H.; Chen, W. Electronic Metal−Support Interaction Modulates Single-Atom Platinum Catalysis for Hydrogen Evolution Reaction. *Nat. Commun.* **2021**, *12* (1), No. 3021.

(17) Biernesser, A. B.; Li, B.; Byers, J. A. Redox-Controlled Polymerization of Lactide Catalyzed by Bis(Imino)Pyridine Iron Bis(Alkoxide) Complexes. *J. Am. Chem. Soc.* **2013**, *135* (44), 16553−16560.

(18) Biernesser, A. B.; Chiaie, K. R. D.; Curley, J. B.; Byers, J. A. Block Copolymerization of Lactide and an Epoxide Facilitated by a Redox Switchable Iron-Based Catalyst. *Angew. Chem., Int. Ed.* **2016**, *55* (17), 5251−5254.

(19) Qi, M.; Dong, Q.; Wang, D.; Byers, J. A. Electrochemically Switchable Ring-Opening Polymerization of Lactide and Cyclohexene Oxide. *J. Am. Chem. Soc.* **2018**, *140* (17), 5686−5690.

(20) Qi, M.; Zhang, H.; Dong, Q.; Li, J.; Musgrave, R. A.; Zhao, Y.; Dulock, N.; Wang, D.; Byers, J. A. Electrochemically Switchable Polymerization from Surface-Anchored Molecular Catalysts. *Chem. Sci.* **2021**, *12* (26), 9042−9052.
(21) Lin, Y.; Zhou, S.; Liu, X.; Sheehan, S.; Wang, D. TiO2/TiSi2 Heterostructures for High-Efficiency Photoelectrochemical H2O Splitting. *J. Am. Chem. Soc.* **2009**, *131* (8), 2772−2773.
(22) Yamashita, T.; Hayes, P. Analysis of XPS Spectra of Fe2+ and Fe3+ Ions in Oxide Materials. *Appl. Surf. Sci.* **2008**, *254* (8), 2441−2449.

https://doi.org/10.1021/acscatal.4c05947
ACS Catal. 2024, 14, 18535−18541